Geochemical Perspectives Letters

Redox dynamics of subduction revealed by arsenic in serpentinite

G.S. Pokrovski[1*], C. Sanchez-Valle[2], S. Guillot[3], A.Y. Borisova[1,8], M. Muñoz[4], A.-L. Auzende[3], O. Proux[5], J. Roux[6], J.-L. Hazemann[7], D. Testemale[7], Y.V. Shvarov[8]

OPEN ACCESS

https://doi.org/10.7185/geochemlet.2225

Abstract

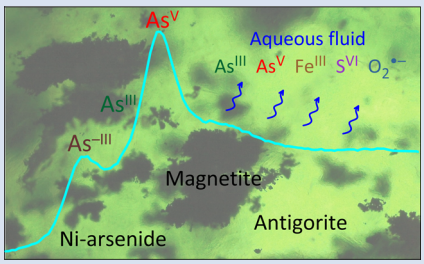

Redox dynamics of subduction processes remain poorly constrained owing to the lack of direct geochemical tracers. We studied, using X-ray absorption spectroscopy, the chemical and redox state of arsenic in the Tso Morari serpentinites that are witnesses of the Himalayan subduction. Our measurements reveal remarkably contrasting redox speciation, from arsenide (As^{-III}) to arsenite (As^{III}) and arsenate (As^{V}). Combined with physical-chemical constraints, these data enable reconstruction of the 'redox travel' of arsenic in the subduction process. Upon early serpentinisation of mantle peridotite, arsenic was scavenged from the fluid and dragged down as insoluble nickel arsenide. Partial deserpentinisation close to the peak metamorphism (550–650 °C) resulted in oxidative dissolution of arsenide to aqueous As^{III} and As^{V} and their non-specific intake by antigorite. The As^{V}/As^{III} ratios (~0.1–10) analysed in the mineral are ~10^4 times higher on average than predicted assuming bulk system thermodynamic equilibrium. These findings reflect a transient out-of-equilibrium release of highly oxidised fluids, with f_{O_2} reaching ~10 log units above the fayalite-magnetite-quartz buffer (FMQ+10). Arsenic in serpentinite is thus a sensitive record of subduction redox dynamics inaccessible when using traditional equilibrium approaches applied to bulk fluid-mineral systems.

Received 4 February 2022 | Accepted 19 May 2022 | Published 14 July 2022

Introduction

Serpentinite formation and breakdown are major phenomena occurring in subduction zones. Knowledge of the redox conditions (f_{O_2}) in these processes is necessary to interpret the transfers of many major and trace elements existing in multiple oxidation states. Most natural, experimental, and modelling studies have tackled redox evolution during subduction using major redox sensitive elements such as C, S, and Fe, but little attention has been devoted to trace elements. Among them, arsenic may be a promising redox indicator because it exhibits a wide range of formal oxidation states, from –III to +V, yielding a variety of minerals from (sulf)arsenides to arsenates, and oxyhydroxide As^{III} and As^{V} species in fluids that may be scavenged or released by major minerals and silicate melts depending on f_{O_2} (*e.g.*, Noll *et al.*, 1996; O'Day, 2006; Perfetti *et al.*, 2008; Borisova *et al.*, 2010; Testemale *et al.*, 2011; Scambelluri *et al.*, 2019).

The present study thus examines the potential of arsenic for tracing subduction zone redox conditions through measurement of arsenic oxidation state and speciation in the Tso Morari serpentinites (NW Himalaya). These rocks were formed by hydration of forearc mantle peridotites by slab-derived fluids and subducted to depth of ~100 km and temperatures of ~650 °C before having been exhumed during the Himalayan orogenesis (Hattori and Guillot, 2007 and references therein). The serpentinites, constituted mostly of antigorite and magnetite (Fig. 1), are highly enriched in As^{V} and As^{III} (up to ~100 ppm As, which is ~1000 times more than in mantle-derived rocks; Hattori *et al.*, 2005; Witt-Eickschen *et al.*, 2009). Combined with the well constrained geodynamic history of the Himalayan subduction (Supplementary Information), these serpentinites represent an excellent natural case to examine the redox cycle of arsenic in a palaeo-subduction zone across a wide range of temperatures (T) and pressures (P).

We used synchrotron X-ray absorption spectroscopy (XAS), which is the most direct method to probe a trace element redox state, chemical bonding and coordination at the atomic scale. Arsenic K-edge X-ray absorption near-edge structure (XANES) and extended X-ray absorption fine structure (EXAFS) spectra were acquired on a thoroughly characterised set of serpentinite rock samples as well as their antigorite- and magnetite-enriched mineral fractions (Supplementary Information; Table S-1). Combined with simulations of

1. Géosciences Environnement Toulouse, Université Toulouse III, GET-CNRS-OMP-UPS-IRD-CNES, 31400 Toulouse, France
2. Institute of Mineralogy, University of Münster, 48149 Münster, Germany
3. Université Grenoble Alpes, Université de Savoie Mont Blanc, CNRS, IRD, Univ. Gustave Eifel, ISTerre, 38000 Grenoble, France
4. Géosciences Montpellier, Université de Montpellier, CNRS, 34095 Montpellier, France
5. Observatoire des Sciences de l'Univers de Grenoble, CNRS-Université Grenoble Alpes, 38400 Saint Martin d'Hères, France
6. Institut de Physique du Globe de Paris, CNRS, 75005 Paris, France
7. Université Grenoble Alpes, CNRS, Grenoble INP, Institut Néel, 38000 Grenoble, France
8. Lomonosov Moscow State University, 119991 Moscow, Russia
* Corresponding author (email: gleb.pokrovski@get.omp.eu; glebounet@gmail.com)

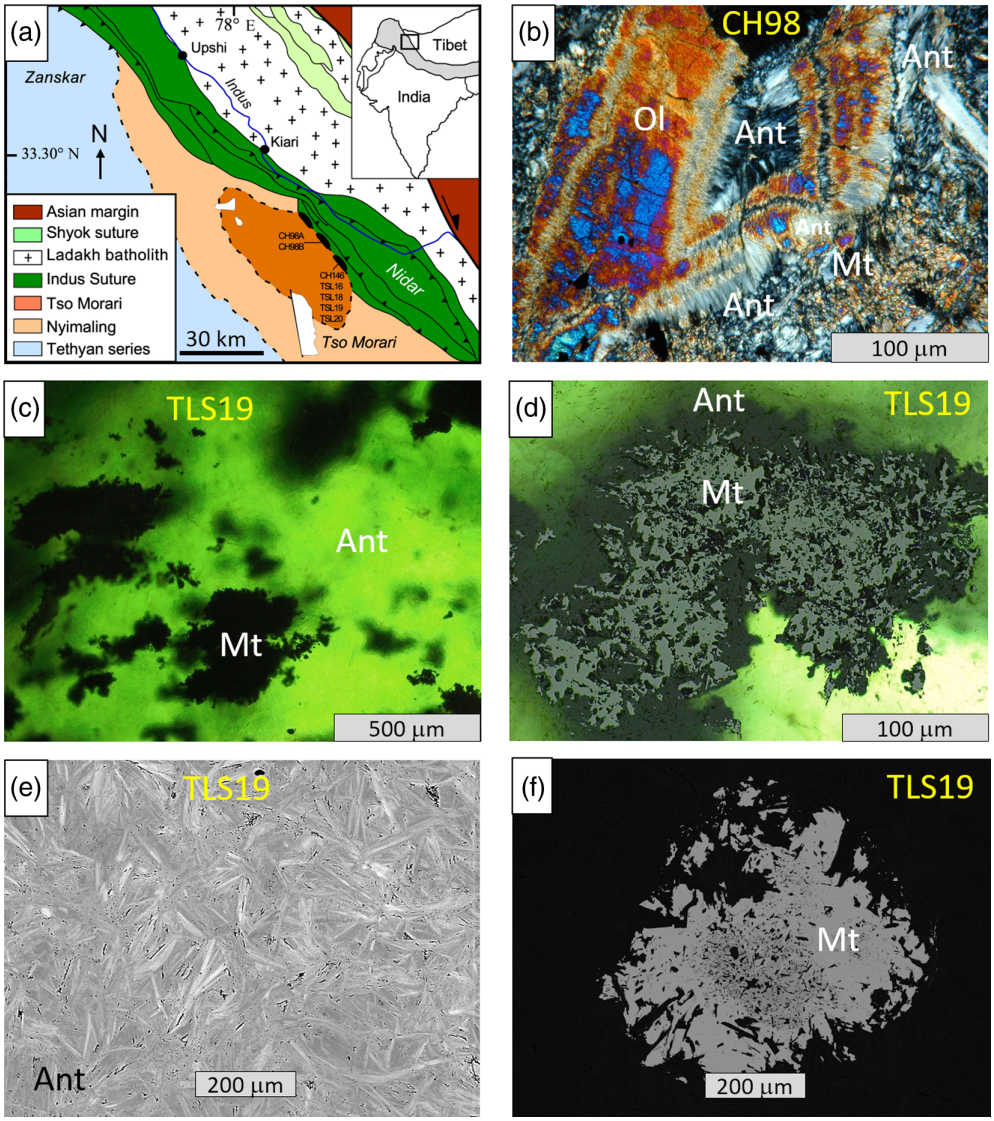

Figure 1 Geology and mineralogy of the Tso Morari serpentinite samples. **(a)** Geological map showing sampling locations. **(b)** Typical serpentinite sample (polarised light) showing dominant antigorite (Ant), metamorphic olivine (Ol) and subordinate magnetite (Mt). **(c)** and **(d)** Magnetite grains embedded in antigorite matrix. **(e)** and **(f)** Antigorite matrix with slight variations in Mg-Al-Si-Fe content and typical magnetite grain displaying Cr-rich core and resorption features (backscattered electron mode). See Supplementary Information for samples identity and characteristics.

fluid-rock interactions using robust thermodynamic data for As-bearing minerals and aqueous species, the results allow us to propose a novel redox model of arsenic behaviour enabling it to unveil f_{O_2} dynamics in subduction processes.

Arsenic Redox and Structural State in Serpentinites

XANES spectra reveal a large range of arsenic redox forms coexisting in serpentinite samples (Fig. 2). Arsenate ($As^{V}O_4$ tetrahedral coordination) is generally the dominant form both in serpentinite and its antigorite fraction (>95 % Ant) with an average of 55 ± 20 mol % (1 s.d.) of total As. The magnetite-enriched fraction (~90 % Mt + 10 % Ant) contains even more As^{V} (from 85 to >95 mol %; Table S-2); however, it accounts for a minor part of As^{V} in the total As budget in serpentinite (Supplementary Information). Arsenate in both minerals coexists with arsenite ($As^{III}O_3$ trigonal pyramidal coordination, from <5 to 55 mol % total As), as well as with arsenide (formal redox state As^{-III}, <5 to 47 mol % total As) in some antigorite samples. EXAFS analyses confirm these findings by showing a mixture of $As^{III}O_3$ and $As^{V}O_4$ first shell coordinations for arsenide-free antigorite and magnetite (*e.g.*, TSL16), and the simultaneous presence of Ni and O in the first atomic shell of As in antigorite samples containing both arsenide and arsenate, showing a mixture of $As^{-III}Ni_6$ and $As^{V}O_4$ coordination environments (*e.g.*, TLS19; Table S-3, Fig. S-1). Nickel arsenide nanoparticles were directly identified by transmission electron microscopy (TEM) in such samples whereas neither As^{III} nor As^{V} individual solid phases were detected (Fig. S-2). The very weak (if any) arsenic second shell EXAFS signals, along with the lack of correlations of As redox state and total contents with those of Fe or other subordinate elements (*e.g.*, Na, Al, V, Co, Ni) that commonly enter magnetite or antigorite structural sites, do not support substitution of As^{III} and As^{V} in $(Si,Fe^{III})O_4$ tetrahedral or $(Mg,Al,Fe^{II,III})O_6$ octahedral sites of both minerals (Supplementary Information). Indeed, the $[As^{III}O_3]$ geometry

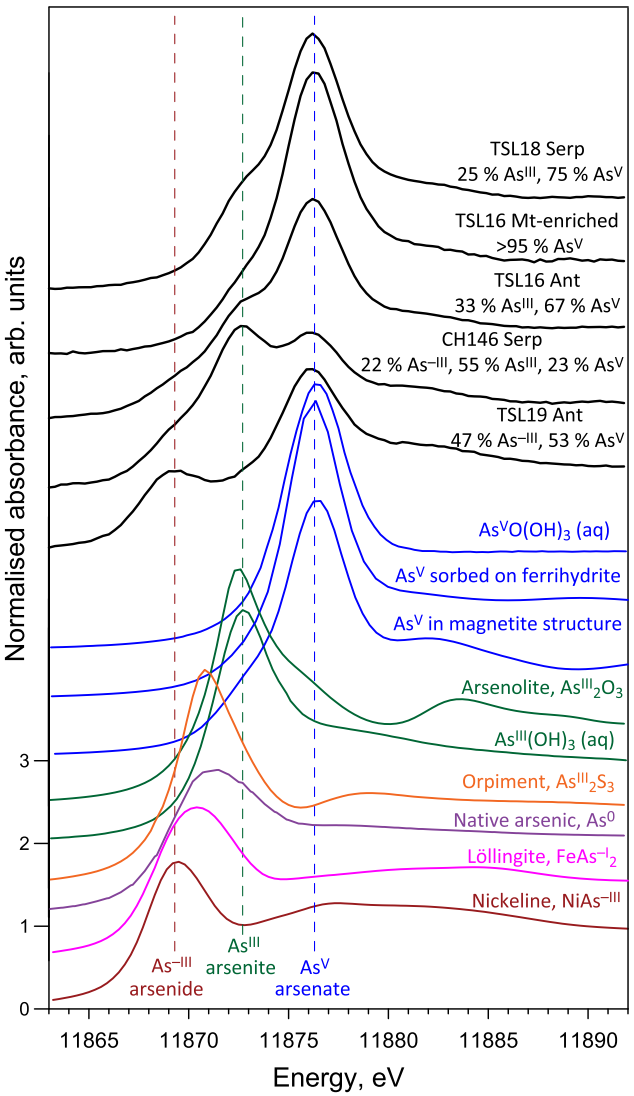

Figure 2 Representative As K-edge XANES spectra acquired on whole rock serpentinite (Serp) and its antigorite (Ant) and magnetite (Mt) enriched fractions, showing contributions of different arsenic formal redox states derived by linear combination fits using different sets of reference solid and aqueous (aq) compounds. Vertical dashed lines indicate the energy positions of the identified arsenic redox states. The best match of all serpentinite spectra was provided by a combination of the spectra of nickeline and aqueous arsenious and arsenic acid species or As^{III} and As^{V} adsorbed on Al/Fe-bearing mineral surfaces. In contrast, our spectra are poorly matched by that of arsenolite, displaying characteristic features arising from As^{III}-O-As^{III} bonds (at 11876 and 11884 eV), and that of As^{V} partially incorporated in magnetite and coordinated by multiple Fe atoms *via* As^{V}-O-Fe bonds (*e.g.*, feature at 11882 eV). See Table S-2 for full dataset and reference compounds, Figure S-1 for EXAFS spectra, and Supplementary Information text for more detailed comparisons.

(Fig. S-1) is structurally incompatible with those sites. The $[As^{V}O_4]^{3-}$ tetrahedron is also incompatible with octahedral sites in Mg/Fe layers and would induce strain and charge imbalance if substituted for smaller and higher charged $[Si^{IV}O_4]^{4-}$ in Si layers of antigorite. Therefore, our data collectively point to site unspecific intake of both As^{III} and As^{V}, likely in structural imperfections common in between Mg-Si layers of antigorite, as oxyhydroxide anions of arsenious and arsenic acid similar to those dominant in aqueous solution (*e.g.*, Perfetti *et al.*, 2008; Testemale *et al.*, 2011).

Arsenic Redox Cycle during Subduction

The presence of contrasting arsenic oxidation states revealed in this study strongly suggests that the serpentinites have undergone large redox changes in *T-P*-time space during subduction. Using equilibrium thermodynamics, we simulated arsenic speciation and solubility during interactions of hydrous sediments (pelite ± seawater) with the mantle wedge (harzburgite) in variable proportions, followed by subduction of the produced serpentinite either in closed or open (*i.e.* partial fluid loss) systems (Fig. 3, Tables S-5, S-6), along the geothermal path established for the Tso Morari metamorphic rocks (Guillot *et al.*, 2008).

We found that, independently of the initial redox state of arsenic, introduced with sediments or water either as sulfarsenide or arsenate, poorly soluble nickel arsenides such as orcelite (Ni_5As_2) and maucherite (Ni_8As_{11}) are the stable phases across a wide range of water/rock and sediment/harzburgite ratios (0.1–5 and 0.1–0.5), from early stages of serpentinisation (<200 °C) to at least 550 °C (Fig. 3). This *T* range corresponds to f_{O_2} of –7 to –3 log units relative to the conventional fayalite-magnetite-quartz buffer (FMQ–7 to –3), as imposed by reactions of Fe^{II}-bearing olivine and pyroxene with water producing Fe^{II}/Fe^{III}-bearing

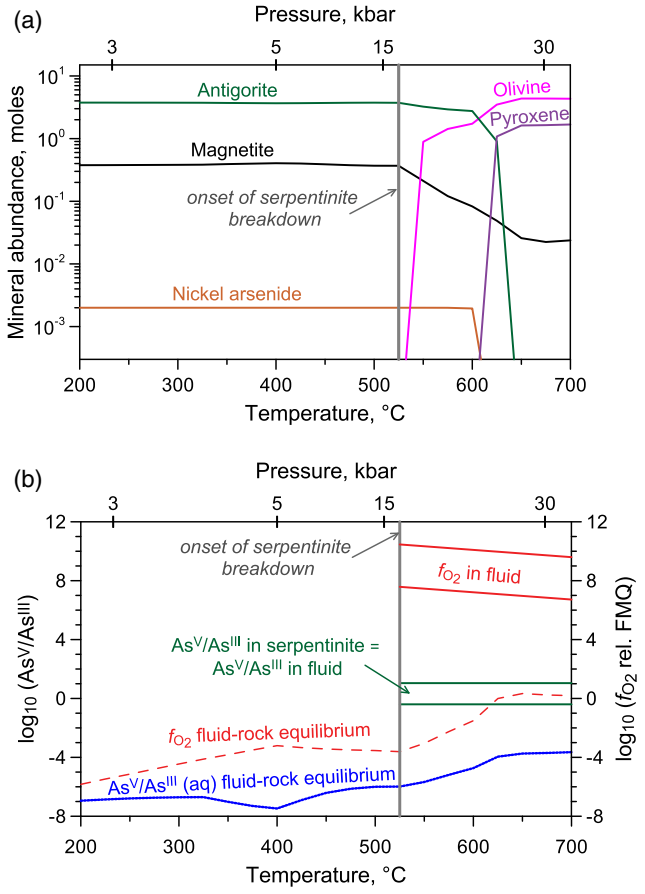

Figure 3 Thermodynamic simulations of serpentinisation in the system harzburgite-sediment-aqueous fluid (starting mass ratios 10:1:10, respectively), along the *T-P* subduction path from Guillot *et al.* (2008). **(a)** Equilibrium relative abundances of key minerals. **(b)** Predicted As^{V}/As^{III} species ratio in the aqueous fluid (dotted blue) and f_{O_2} (dashed red) assuming bulk system equilibrium, as compared to the range of f_{O_2} in the fluid (lower and higher bounds, solid red) corresponding to the range of As^{V}/As^{III} ratios measured in serpentinite (solid green).

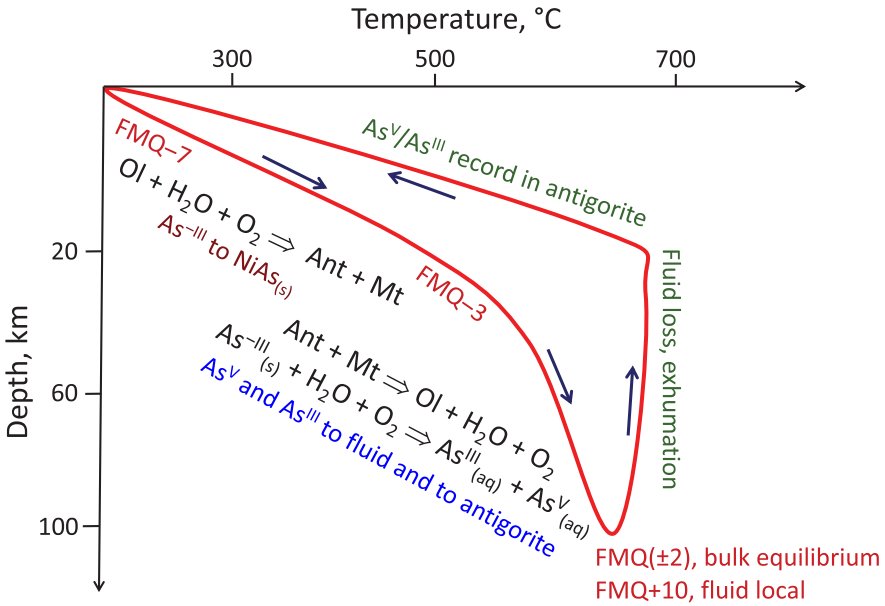

Figure 4 Arsenic redox transformation reactions along the *T vs.* depth subduction path of the Tso Morari metamorphic rocks. Arrows show the directions of the subduction and subsequent exhumation. Ant = antigorite, Mt = magnetite, Ol = olivine.

antigorite and magnetite while consuming oxygen (Fig. 4). The predicted aqueous arsenic concentrations are <1 ppb below 500 °C (Fig. S-5a), demonstrating that arsenic was not a fluid mobile element and was hosted by Ni arsenide phases, in full agreement with the XAS and TEM analyses (Figs. 2, S-2). Highly reducing conditions inherent to this subduction step are also supported by findings of methane-bearing inclusions in partly serpentinised olivine of the Nidar ophiolite complex adjacent to Tso Morari (Fig. 1a; Sachan *et al.*, 2007). Reducing environments at the serpentinisation step are equally common in other subduction settings, for instance as evidenced by Fe-Ni arsenides in Kamchatka peridotite xenoliths altered by slab-derived fluids (Ishimaru and Arai, 2008), and by graphite in the Alpine blueschist-to-eclogite facies (Malvoisin *et al.*, 2012). It is only above 550 °C, with onset of partial breakdown of antigorite and magnetite to olivine, that the solubility of the arsenide phases in the fluid as dominantly As^{III} oxyhydroxide species does significantly increase (Fig. S-5a). This simulated scenario is consistent with the textures and compositional variations of magnetite observed in our samples likely reflecting recrystallisation/replacement phenomena (Fig. 1f) as well as the lack of arsenide phases in some of our samples (Figs. 2, S-2).

Our modelling does not support the hypothesis of early intake of As^V by serpentinite (Hattori *et al.*, 2005), which is inconsistent with low f_{O_2} values at early serpentinisation steps (<FMQ–3; Figs. 3, S-5). Such highly reducing conditions are also supported by ubiquitous experimental evidence of H_2 production upon ultramafic rock hydration as well as the occurrence of reduced accessory minerals (sulfarsenides, Fe-Ni alloys) in serpentinisation reactions both in nature and laboratory (*e.g.*, Frost, 1985; McCollom and Bach, 2009; Marcaillou *et al.*, 2011; González-Jiménez *et al.*, 2021). Oxidation to As^V during exhumation is equally unlikely because it would have required either influx of extremely oxidising fluids (*i.e.* $f_{O_2} \approx$ FMQ+10) not evidenced during the inferred hydration events (Palin *et al.*, 2014), or direct near surface oxidation and weathering. Both phenomena would have produced hematite/goethite and clays not observed in the Tso Morari rocks (Hattori and Guillot, 2007; Deschamps *et al.*, 2010). Therefore, arsenic redox captured by serpentinite likely reflects subduction phenomena at depth.

Release of Highly Oxidised Fluids in Subduction Zones Revealed by Arsenic Redox

In light of our results demonstrating the absence of selective site specific As^V and As^{III} incorporation in serpentine, no significant As^V *vs.* As^{III} fractionation would be induced upon arsenic intake, thereby making the As^V/As^{III} ratio in the mineral to be representative of that in the coexisting aqueous fluid. The thermodynamically predicted As^V/As^{III} ratios (10^{-6} to 10^{-3}) in the fluid phase in the 550–650 °C range of the deserpentinisation step under redox conditions of bulk system equilibrium are, however, much lower than the ratios measured in our antigorite and magnetite-enriched samples (from 0.4 to >11; Fig. 3b, Table S-1). Assuming that all dissolved species including As^V and As^{III} rapidly re-equilibrate in aqueous solution at such elevated *T*, the measured As^V/As^{III} ratios in antigorite would correspond to f_{O_2} values of FMQ+8 to +12 in the fluid, which are ~10 log units higher than those calculated in the bulk fluid-mineral system at equilibrium (~FMQ; Fig. 4). This difference is beyond reasonable error margins of our f_{O_2} estimates (±2 log units; Supplementary Information), and therefore reflects out-of-equilibrium oxidised fluid release during partial serpentinite decomposition, according to the formal reactions shown in Figure 4. Note that even though our f_{O_2} estimates are close to mbar levels of partial P_{O_2}, the equivalent concentration of the aqueous molecular O_2^0 species at these *T-P* conditions is only ~10^{-10} molal. Therefore, the oxidation potential of the released fluid is mostly carried by more concentrated dissolved elements in their highest oxidation states, such as As^V, Fe^{III} and S^{VI} and, possibly, by reactive oxygen species like $O_2^{\bullet-}$ or H_2O_2. However, given the large predominance of both Fe^{II} and Fe^{III} in serpentinite rock, the amount of all dissolved redox sensitive elements (Fe, As, S, O) in the fluid (Fig. S-5) would be insufficient to significantly alter the Fe redox ratio of the major solid phases and, consequently, to leave clearly

detectable Fe redox imprint in the rock. Locally focused oxidised fluid release in the proximity of resorbing magnetite grains (Fig. 1) would also explain the more elevated As^{V}/As^{III} ratios (~10) found in magnetite-enriched fractions than in antigorite fractions (~1).

The f_{O_2} values derived from arsenic redox are significantly higher than those estimated based on Fe oxy-thermobarometry of metamorphic minerals associated with deep subduction (*e.g.*, garnet, spinel, pyroxene, amphibole; Cannaò and Malaspina, 2018; Gerrits *et al.*, 2019), equilibrium thermodynamic simulations of fluid-rock interactions in this and previous work (*e.g.*, Debret and Sverjensky, 2017; Piccoli *et al.*, 2019; Evans and Frost, 2021), and antigorite dehydration experiments (Maurice *et al.*, 2020). Their f_{O_2} estimations commonly range from FMQ to FMQ+5, with an upper limit being close to the hematite-magnetite equilibrium. Our arsenic-derived f_{O_2} values of FMQ+8 to +12 in the absence of hematite thus clearly indicate out-of-equilibrium release of highly oxidised fluids that is not captured by iron as the overwhelmingly dominant redox sensitive element in serpentinite. Interestingly, comparably high f_{O_2} values were inferred from manganese-bearing metacherts in subduction mélanges (Tumiati *et al.*, 2015), pointing to potentially wide occurrence of phenomena of oxidised fluid generation.

Our findings thus provide novel insight into the redox dynamics and geochemical cycles in subduction zones. Like for arsenic, the transfer of other metalloids (*e.g.*, P, Sb, Se, Te) in subduction zones may be fundamentally controlled by f_{O_2}, spanning over >15 orders of magnitude relative to FMQ across subduction, from early reducing conditions stabilising poorly soluble Fe/Ni phases of these elements, to highly oxidising conditions promoting their soluble oxyanions. More generally, our results highlight an important divide between the redox potential of a bulk serpentine rock (Tumiati *et al.*, 2015; Evans and Frost, 2021; Galvez and Jaccard, 2021) and that of the out-of-equilibrium aqueous fluid phase generated therefrom. Such highly oxidised fluids may selectively carry major redox sensitive elements in their highest valence states (Fe^{III}, Mn^{IV}, sulfate, carbonate), in contrast to equilibrium thermodynamic predictions in rock buffered systems that suggest reduced valence states of these elements to be equally (or more) abundant in the fluid. Our findings may thus provide new constrains on the speciation and transfer of metals and volatiles and their associated stable isotope signatures (*e.g.*, Debret *et al.*, 2016; Walters *et al.*, 2019) and, more globally, on the dynamics of redox reactions at depth.

Acknowledgements

This work was funded by the Institut des Sciences de l'Univers of the Centre National de la Recherche Scientifique (INSU ASEDIT), the Partenariat Hubert Curien (PHC Germaine de Staël), the Agence Nationale de la Recherche (RadicalS ANR-16-CE31-0017), and the Institut Carnot (ISIFoR OrPet and AsCOCrit). The European Synchrotron Radiation Facility (ESRF) provided access to beam time and infrastructure. The FAME facility is supported by the CEA-CNRS-CRG consortium and the INSU. We thank A.-M. Cousin for help with figure layout, F. Maube and L. Menjot for SEM and XRD analyses, G. Morin, J. Rose, A. Foster, and C. van Genuchten for sharing XAS references, M. Galvez, M. Blanchard, M. Brounce and an anonymous reviewer for comments, and S. Myneni for editorial handling.

Editor: Satish Myneni

Additional Information

Supplementary Information accompanies this letter at https://www.geochemicalperspectivesletters.org/article2225.

Cite this letter as: Pokrovski, G.S., Sanchez-Valle, C., Guillot, S., Borisova, A.Y., Muñoz, M., Auzende, A.-L., Proux, O., Roux, J., Hazemann, J.-L., Testemale, D., Shvarov, Y.V. (2022) Redox dynamics of subduction revealed by arsenic in serpentinite. *Geochem. Persp. Let.* 22, 36–41. https://doi.org/10.7185/geochemlet.2225

References

Borisova, A.Y., Pokrovski, G.S., Pichavant, M., Fredier, R., Candaudap, F. (2010) Arsenic enrichment in hydrous peraluminous melts: Insights from femtosecond laser ablation-inductively coupled plasma-quadrupole mass spectrometry, and in situ X-ray absorption fine structure spectroscopy. *American Mineralogist* 95, 1095–1104. https://doi.org/10.2138/am.2010.3424

Cannaò, E., Malaspina, N. (2018) From oceanic to continental subduction: Implications for the geochemical and redox evolution of the suprasubduction mantle. *Geosphere* 14, 2311–2336. https://doi.org/10.1130/GES01597.1

Debret, B., Sverjensky, D.A. (2017) Highly oxidising fluids generated during serpentinite breakdown in subduction zones. *Scientific Reports* 7, 10351. https://doi.org/10.1038/s41598-017-09626-y

Debret, B., Millet, M.-A., Pons, M.-L., Bouilhol, P., Inglis, E., Williams, H. (2016) Isotopic evidence of iron mobility during subduction. *Geology* 44, 215–218. https://doi.org/10.1130/G37565.1

Deschamps, F., Guillot, S., Godard, M., Chauvel, C., Andreani, M., Hattori, K.H. (2010) In situ characterization of serpentinites from forearc mantle wedges: timing of serpentinization and behavior of fluid-mobile elements in subduction zones. *Chemical Geology* 269, 262–277. https://doi.org/10.1016/j.chemgeo.2009.10.002

Evans, K.A., Frost, B.R. (2021) Deserpentinization in subduction zones as a source of oxidation in arcs: a reality check. *Journal of Petrology* 62, egab016. https://doi.org/10.1093/petrology/egab016

Frost, B.R. (1985) On the stability of sulfides, oxides and native metals in serpentinite. *Journal of Petrology* 26, 31–63. https://doi.org/10.1093/petrology/26.1.31

Galvez, M.E., Jaccard, S.L. (2021) Redox capacity of rocks and sediments by high temperature chalcometric titration. *Chemical Geology* 564, 120016. https://doi.org/10.1016/j.chemgeo.2020.120016

Gerrits, A.R., Inglis, E.C., Dragovic, B., Starr, P.G., Baxter, E.F., Burton, K.W. (2019) Release of oxidizing fluids in subduction zones recorded by iron isotope zonation in garnet. *Nature Geoscience* 12, 1029–1033. https://doi.org/10.1038/s41561-019-0471-y

González-Jiménez, J.M., Piña, R., Saunders, J.E., Plissart, G., Marchesi, C., Padrón-Navarta, J.A., Ramón-Fernandez, M., Garrido, L.N.F., Gervilla, F. (2021) Trace element fingerprints of Ni–Fe–S–As minerals in subduction channel serpentinites. *Lithos* 400–401, 106432. https://doi.org/10.1016/j.lithos.2021.106432

Guillot, S., Mahéo, G., de Sigoyer, J., Hattori, K.H., Pêcher, A. (2008) Tethyan and Indian subduction viewed from the Himalayan high- to ultrahigh-pressure metamorphic rocks. *Tectonophysics* 451, 225–241. https://doi.org/10.1016/j.tecto.2007.11.059

Hattori, K.H., Guillot, S. (2007) Geochemical character of serpentinites associated with high- to ultrahigh-pressure metamorphic rocks in the Alps, Cuba, and the Himalayas: recycling of elements in subduction zones. *Geochemistry, Geophysics, Geosystems* 8, 1–27. https://doi.org/10.1029/2007GC001594

Hattori, K., Takahashi, Y., Guillot, S., Johanson, B. (2005) Occurrence of arsenic (V) in forearc mantle serpentinites based on X-ray absorption spectroscopy study. *Geochimica et Cosmochimica Acta* 69, 5585–5596. https://doi.org/10.1016/j.gca.2005.07.009

Ishimaru, S., Arai, S. (2008) Arsenide in a metasomatized peridotite xenolith as a constraint on arsenic behavior in the mantle wedge. *American Mineralogist* 93, 1061–1065. https://doi.org/10.2138/am.2008.2746

Malvoisin, B., Chopin, C., Brunet, F., Galvez, M.E. (2012) Low-temperature wollastonite formed by carbonate reduction: a marker of serpentinite redox conditions. *Journal of Petrology* 53, 159–176. https://doi.org/10.1093/petrology/egr060

Marcaillou, C., Muñoz, M., Vidal, O., Parra, T., Harfouche, M. (2011) Mineralogical evidence for H_2 degassing during serpentinization at 300 °C/300 bar. *Earth and Planetary Science Letters* 303, 281–290. https://doi.org/10.1016/j.epsl.2011.01.006

Maurice, J., Bolfan-Casanova, N., Demouchy, S., Chauvigne, P., Schiavi, F., Debret, B. (2020) The intrinsic nature of antigorite breakdown at 3 GPa: Experimental constraints on redox conditions of serpentinite dehydration in subduction zones. *Contributions to Mineralogy and Petrology* 175, 94. https://doi.org/10.1007/s00410-020-01731-y

McCollom, T.M., Bach, W. (2009) Thermodynamic constraints on hydrogen generation during serpentinization of ultramafic rocks. *Geochimica et Cosmochimica Acta* 73, 856–875. https://doi.org/10.1016/j.gca.2008.10.032

Noll, P.D. Jr., Newsom, H.E., Leeman, W.P., Ryan, J.R. (1996) The role of hydrothermal fluids in the production of subduction zone magmas: Evidence from siderophile and chalcophile trace elements and boron. *Geochimica et Cosmochimica Acta* 60, 587–611. https://doi.org/10.1016/0016-7037(95)00405-X

O'Day, P.A. (2006) Chemistry and mineralogy of arsenic. *Elements* 2, 77–83. https://doi.org/10.2113/gselements.2.2.77

Palin, R.M., St-Onge, M.R., Waters, D.J., Searle, M.P., Dyck, B. (2014) Phase equilibria modelling of retrograde amphibole and clinozoisite in mafic eclogite from the Tso Morari massif, northwest India: constraining the *P–T–M* (H_2O) conditions of exhumation. *Journal of Metamorphic Geology* 32, 675–693. https://doi.org/10.1111/jmg.12085

Perfetti, E., Pokrovski, G.S., Ballerat-Busserolles, K., Majer, V., Gibert, F. (2008) Densities and heat capacities of aqueous arsenious and arsenic acid solutions to 350 °C and 300 bar, and revised thermodynamic properties of As$(OH)_3^0$(aq), AsO$(OH)_3^0$(aq) and iron sulfarsenide minerals. *Geochimica et Cosmochimica Acta* 72, 713–731. https://doi.org/10.1016/j.gca.2007.11.017

Piccoli, F., Hermann, J., Pettke, T., Connoly, J.A.D., Kempf, E.D., Vieira Duarte, J.F. (2019) Subducting serpentinites release reduced, not oxidized, aqueous fluids. *Scientific Reports* 9, 19573. https://doi.org/10.1038/s41598-019-55944-8

Sachan, H.K., Mukherjee, B.K., Bodnar, R.J. (2007) Preservation of methane generated during serpentinization of upper mantle rocks: Evidence from fluid inclusions in the Nidar ophiolite, Indus Suture Zone, Ladakh (India). *Earth and Planetary Science Letters* 257, 47–59. https://doi.org/10.1016/j.epsl.2007.02.023

Scambelluri, M., Cannaò, E., Gilio, M. (2019) The water and fluid-mobile element cycles during serpentinite subduction: A review. *European Journal of Mineralogy* 31, 405–428. https://doi.org/10.1127/ejm/2019/0031-2842

Tumiati, S., Godard, G., Martin, S., Malaspina, N., Poli, S. (2015) Ultra-oxidized rocks in subduction mélanges? Decoupling between oxygen fugacity and oxygen availability in a Mn-rich metasomatic environment. *Lithos* 226, 116–130. https://doi.org/10.1016/j.lithos.2014.12.008

Testemale, D., Pokrovski, G.S., Hazemann, J.-L. (2011) Speciation of As^{III} and As^{V} in hydrothermal fluids by in situ X-ray absorption spectroscopy. *European Journal of Mineralogy* 23, 379–390. https://doi.org/10.1127/0935-1221/2011/0023-2104

Walters, J.B, Cruz-Uribe, A.M., Marschall, H.R. (2019) Isotopic compositions of sulfides in exhumed high-pressure terranes: Implications for sulfur cycling in subduction zones. *Geochemistry, Geophysics, Geosystems* 20, 3347–3374. https://doi.org/10.1029/2019GC008374

Witt-Eickschen, G., Palme, H., O'Neill, H.St.C., Allen, C.M. (2009) The geochemistry of the volatile trace elements As, Cd, Ge, In and Sn in the Earth's mantle: New evidence from in situ analyses of mantle xenoliths. *Geochimica et Cosmochimica Acta* 73, 1755–1778. https://doi.org/10.1016/j.gca.2008.12.013